ELSEVIER

Energy and Buildings 29 (1998) 83–92

ENERGY AND BUILDINGS

Reductions in air conditioning energy caused by a nearby park

Vu Thanh Ca *, Takashi Asaeda, Eusuf Mohamad Abu [a]

[a] *Saitama University, Department of Civil and Environmental Engineering, 255 Shima-okubo, Urawa, Saitama 338-8570, Japan*

Received 7 November 1996; accepted 27 May 1998

Abstract

Field observations were carried out to determine the influence of a park on the urban summer climate in the nearby areas. The possibilities of reduction in air conditioning energy were investigated. Air temperature, relative humidity and other meteorological factors were measured at many locations inside a park and in the surrounding areas in the Tama New Town, a city in the west of the Tokyo Metropolitan Area, Japan. The observations indicated that vegetation could significantly alter the climate in the town. At noon, the highest temperature of the ground surface of the grass field in the park was 40.3°C, which was 19°C lower than that of the asphalt surface or 15°C lower than that of the concrete surface in the parking or commercial areas. At the same time, air temperature measured at 1.2 m above the ground at the grass field inside the park was more than 2°C lower than that measured at the same height in the surrounding commercial and parking areas. Soon after sunset, the temperature of the ground surface at the grass field in the park became lower than that of the air, and the park became a cool island whereas paved asphalt or concrete surfaces in the town remained hotter than the overlying air even late at night. With a size of about 0.6 km^2, at noon, the park can reduce by up to 1.5°C the air temperature in a busy commercial area 1 km downwind. This can lead to a significant decrease of in air conditioning energy in the commercial area. © 1998 Elsevier Science S.A. All rights reserved.

Keywords: Air conditioning energy; Urban thermal environment; Thermal comfort; Vegetation

1. Introduction

It is well-known that the development of cities significantly changes the climate of the city and surrounding areas. The increase in the impervious portion of the ground surface in the urban area caused by pavements, roads and buildings significantly reduces evaporation from the ground surface, and consequently increases the underground heat storage. This underground heat storage makes the ground surface temperature higher than that of the previously vegetated surface, thus increasing the sensible heat exchange between the ground surface and the atmosphere, and the upward long wave radiation. On the other hand, tall buildings with shading effect in the ground/wall surfaces may cause a reduction in air temperature at noon. However, even with the shading effect, in many cases, the heat released from the hot surfaces together with anthropogenic heat released from industry and human activity make the air temperature in the urban area significantly higher than that in the surrounding rural areas, causing the so called 'urban heat island' (Oke [12], Asaeda and Vu [1], Harazono et al. [7]). The intensity of the urban heat island, defined as the difference in air temperature between the city and surrounding rural areas, is more significant at night.

With increasing urbanization, the urban heat island will affect a larger number of urban residents. Thus in areas where there is thermal stress, it makes sense to develop ecological approaches to mitigation.

It has been reported that green areas in cities not only improve the urban landscape, but also can regulate the urban climate by increasing the moisture content in the air and reducing the urban air temperature (Harazono et al. [7], Honjo and Takakura [8]). With the presence of a vegetated surface, evapotranspiration can transform a large portion of incoming solar radiation to the surface, which otherwise would contribute to the underground heat storage, into latent heat and makes the ground surface cooler. Thus in making a development plan of a city, the effect of vegetation on the urban thermal climate should be studied carefully.

Previous studies regarding this problem mainly focus on the effects of green areas on the building thermal climate (Givoni [6], Parker [13–15], Hoyano [9], Harazono et al. [7]). Honjo and Takakura [8] studied thermal effects of urban green areas on their surrounding areas based on a numerical model.

The purpose of this study is to give a detailed investigation on the effects of vegetated areas on the thermal climate of a

* Corresponding author. Tel.: +81 48 8583567; fax: +81 48 8587374; e-mail: vuca@env.civil.saimata-u.ac.jp

0378-7788/98/$ - see front matter © 1998 Elsevier Science S.A. All rights reserved.
PII S0378-7788(98)00032-2

new city in the Tokyo Metropolitan area, the Tama New Town, through field observations of the ground surface temperature, atmospheric temperature and other atmospheric conditions during hot summer days.

2. Observational procedure and equipment

The study area is located within the Tama New Town, a new, well-planned city in the West of the Tokyo Metropolitan area (Fig. 1). The construction of the town began in 1963. At present, the town has an area of 30.2 km^2 with a population of about 410 000. The study area, which is near the Tama Central Station, has a size of about 1.2 km × 1.2 km (Fig. 1). A large portion of the ground surface in the study region is covered by commercial and office buildings together with asphalt paved parking lots. There are several green areas in the region with the largest one at the Tama Central Park as indicated in Fig. 1.

Observations were carried out during the summer season from August to September 1994. During the observations, hourly values of air temperature, relative humidity, wind velocity, foliage temperature, and temperatures of the grass surface, wall and pavement surfaces were measured at many locations in the area by six groups of students riding on bicycles and cars. Solar radiation, downward longwave radiation, net radiation, albedo, together with soil temperature at the ground surface, 5 and 10 cm depths were measured at the center of a wide grass field in the center of the park. Air temperature, relative humidity and wind velocity were also measured at a height of 113.6 m above the ground surface on top of the Fukutake Publishing House building, or 2 m above the roof. The values measured above this building can be considered representative for the study region.

Although observations were carried out several times during the summer of 1994, for the purpose of this study, all observational periods except August 26–27 were rejected because of variable weather. During some observational periods, the weather was fine during the morning, and then became cloudy or rainy in the afternoon. Thus, the data collected were not representative of hot summer days in this area of Japan. As the purpose of this study is to investigate the effect of vegetation on the thermal environment of an urban area, only results obtained during the fine days of August 26–27 when the effects were notable are reported here.

Fig. 1 also depicts the observational points in the study area during August 26–27. Details of the observational locations, items and equipment are shown in Table 1. In this table, 'measured band' in the last column means the sensitive band for wave length.

The sampling interval is 5 min for soil temperature and radiation and 30 min during the day and 1 h at night for the other measurements. It was not possible to have simultaneous measurements at all observational points, and values for a physical quantity at all points at a given time were obtained by interpolation.

For the measurements by students riding on cars, to avoid any possible contamination by engine heat from the car, measurements were taken when the car was stopped and at a distance of more than 5 m in front of the car.

Since various equipment were used for the measurement of air temperature, relative humidity, ground surface temperature and wind velocity at different locations, all equipment were calibrated before and after the observation in the laboratory and the field data were adjusted according to the calibration results.

The data of air temperature and wind velocity on top of the Fukutake publishing house were verified by comparing with data at nearby meteorological observational stations. A general agreement confirms that the obtained data can be considered representative for the observational area.

3. Effects of grass and wooded areas on the heating and cooling

Atmospheric conditions such as solar radiation, atmospheric downward longwave radiation, net downward radiation recorded at the grass field inside the park are depicted in Fig. 2. Fig. 3 depicts relative humidity, air temperature and wind velocity, measured simultaneously at the same place. It can be seen that during the day, the weather was fine with a downward maximum solar radiation flux higher than 780 W/m^2 at 12 a.m. The highest air temperature at the grass field (32.4°C) was recorded at 2 p.m. while the lowest air temperature (23.5°C) was recorded at 6 a.m. Relative humidity reached 100% at night and about 60% at noon. It was relatively calm at night, but the wind became strong from 9 a.m. until 7 p.m. with maximum wind velocity of 7.3 m/s, recorded at 3 p.m., and predominantly from the south.

Fig. 4 depicts the time variation of the temperature at ground surface in the grass field, on a nearby asphalt road and concrete pavement, the temperature under the woods, the foliage temperature above the woods and the temperature of the water in the pond for 24 h, from 00:00 August 26 to 00:00 August 27. The surface temperature of the asphalt road and concrete pavement at noon rose up to 55°C at noon, almost 23°C higher than the air temperature measured at 1.2 m above the surface. At the same time, the grass surface temperature reached a maximum of 40.3°C, only about 8°C higher than the air temperature. The foliage temperature above the woods reached 37.8°C or 5.4°C higher than that of the air above the grass surface, while the air temperature in the woods reached 31.0°C.

Fig. 5 depicts the time variation of temperature at the surface, 5 and 10 cm below the surface of the grass field. During the observational period, there was no water supply to the grass field, which was usually well irrigated. It is clear that even when the surface temperature at the grass surface rose to 40.3°C, the temperature at a depth of 5 cm reached a maximum of only 30.2°C at 3 p.m., and the temperature at 10 cm depth reached a maximum of 28.5°C at 5 p.m. The steep variation of soil temperature with depth near the grass

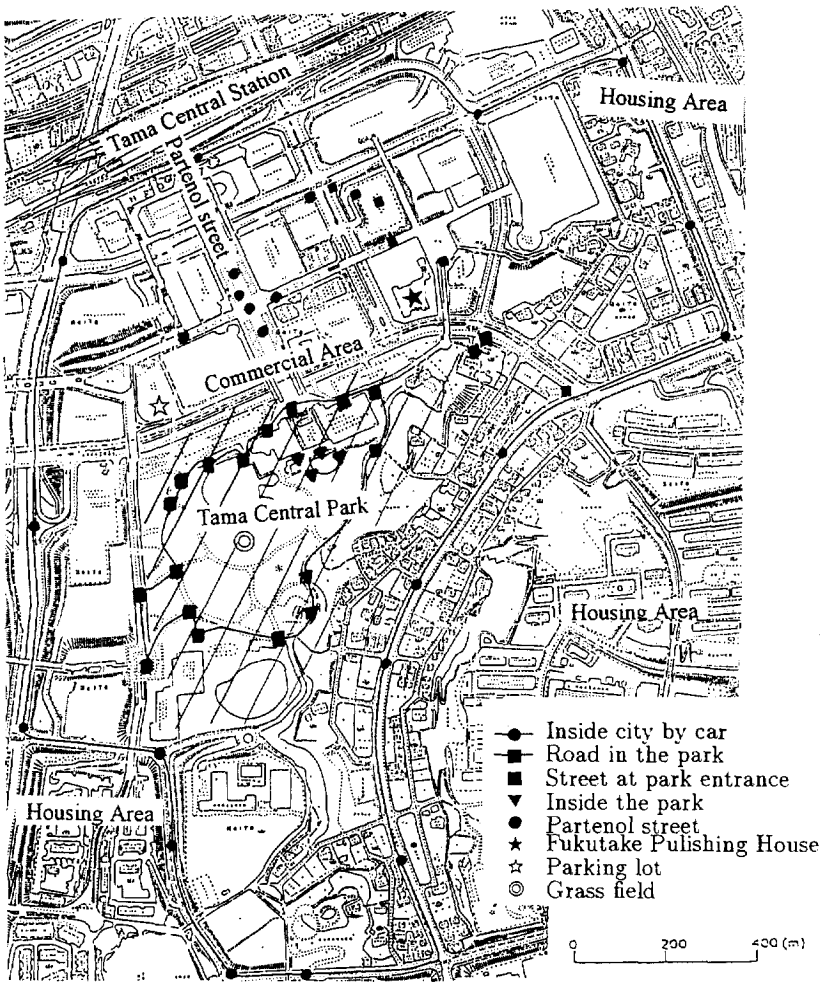

Fig. 1. Map of the study area and observational points.

Table 1
Observational locations, items and equipment

Location	Observational Items	Observational Equipment (accuracy or measured band)
Partenol street	Air temperature, relative humidity wind direction, wind velocity	Digital thermohygrometer (DTH-3, Tokyo Keisoku) (±0.2°C and ±0.5%); Microanemometer (KC-101 Makino Oyo Sokuki Kenkyujo)
Streets in front of the park	Air temperature, relative humidity, temperatures of the sunlit and shaded ground surface, tree foliage, grass surface	Thermohygrometer (TRH-CZ Jinei) (±0.1°C and ±0.5%); Pyranometer (IT2-60, Keyence) (8–16 μm)
Inside city	Air temperature, relative humidity	Digital thermohygrometer (Climomaster Model 651, Kanomax) (±0.1°C and ±0.5%)
2 m above the roof of 111.6 m above ground surface	Air temperature, relative humidity atmospheric pressure, wind velocity and direction	Meteograph No. 8-P (Ota Keiki Seisakusho) (±1°C and ±5%); Anemometer (KC-101, Makino Oyo Sokuki Kenkyujo)
Road in the Park	Air temperature, relative humidity, temperatures of the sunlit and shaded ground surface, tree foliage, grass surface	Thermohygrometer (TRH-CZ, Jinei) (±0.1°C and ±0.5%); Pyranometer (Thermoflow EM-101, Eko) (3–30 μm)
Grass field in the park	Air temperature, relative humidity, wind velocity and direction, downward longwave radiation, Albedo, Net radiation, Solar radiation, Ground temperature at the surface and 5 cm, 10 cm depth, water temperature in a nearby pond	Thermohygrometer (TRH-CZ, Jinei) (±0.1°C and ±0.5%); Anemometer (KC-101, Makino Oyo Sokuki Kenkyujo); Pyrgeometer (MS-200, Eko) (5–50 μm); Albedometer (MR-22, Eko) (0.3–3 μm); Net-radiometer (CN-11, Eko) (0.3–50 μm) Pyranometer (Ota Keiki) (0.36–2 μm); Thermocouple
In the wood	Ground surface temperature, air temperature	Thermography (TVS2000LW) (Nippon Abionix) (8–12 μm); Thermohygrometer (TRH-CZ, Jinei) (±0.1°C and ±0.5%)

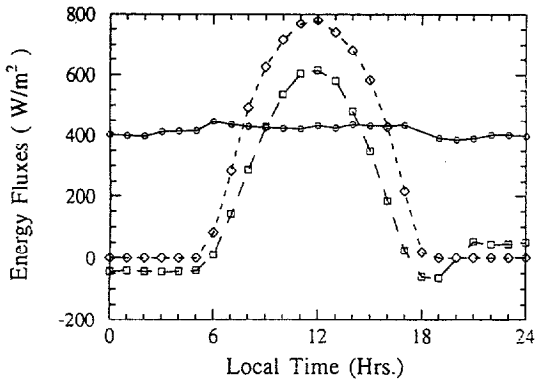

Fig. 2. Radiation conditions at the grass field, ◇ incoming solar radiation, ○ downward infrared longwave radiation, □ downward net total radiation.

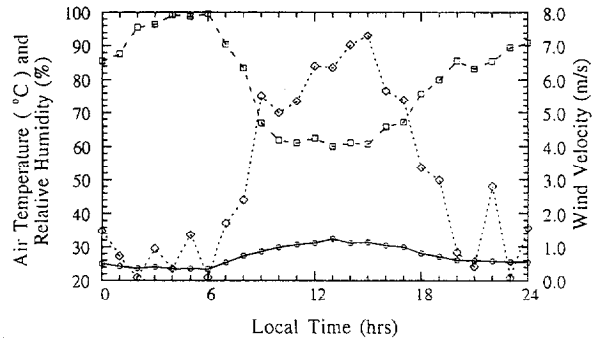

Fig. 3. Meteorological conditions at the grass field, ○ air temperature, □ relative humidity, ◇ wind velocity.

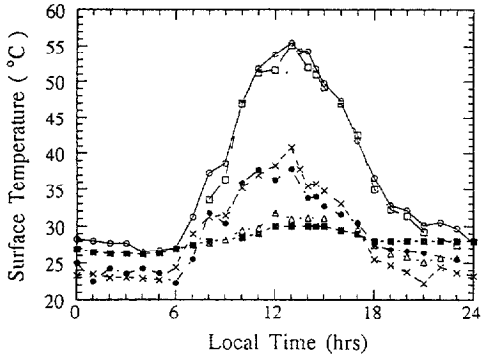

Fig. 4. Time variation of temperature at the – ∘ – asphalt surface, – □ – concrete surface, – × – grass surface, – △ – under the wood, – · – foliage, – – □ – – water surface inside the park.

surface is due to the small thermal conductivity of the soil. This means that for this surface, the heat conducted to deep soil layers, or the below surface heat storage is small. Even before sunset, at 5 p.m., the temperature of the grass surface fell below that of the air and the grass surface began to cool the atmosphere.

Other studies (Asaeda et al. [2], Doll et al. [5]) revealed that in contrast to the grass surface, paved surfaces store a large amount of heat during the day and continue to heat the atmosphere throughout the day and night.

Fig. 6 depicts the time variation of surface temperature of an asphalt paved parking lot inside the commercial area in the north of the park, together with the surface temperature of a nearby grass area, a shaded area, and the foliage temperature. Fig. 7 depicts air temperature and relative humidity measured at the same place at 1.2 m above (the surface). As shown in Fig. 6, the temperature of the asphalt surface reached a maximum of 59°C at about 1 p.m. At the same time, the temperature of the nearby grass surface reached a maximum of only 39.7°C, almost 20°C lower than that of the asphalt surface. The temperature of the leaves reached a maximum value of 39.3°C and fell below that of the air from 5 p.m. onwards. Comparing the air temperature and relative humid-

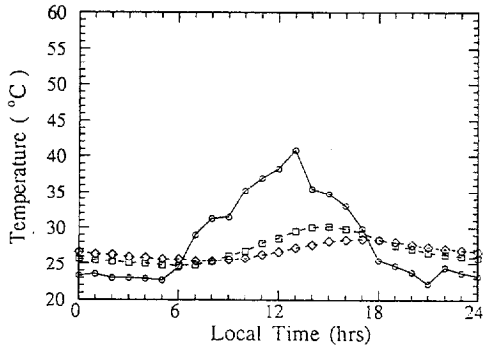

Fig. 5. Time variation of soil temperature at the grass field inside the park, – ∘ – at the soil surface, – □ – 5 cm below surface, – ◇ – 10 cm below surface.

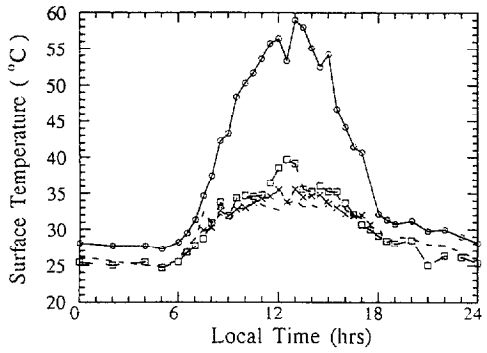

Fig. 6. Time variation of temperature of the – ∘ – asphalt surface, – □ – grass surface, - - - foliage, – × – shaded surface at the parking lot in the commercial area.

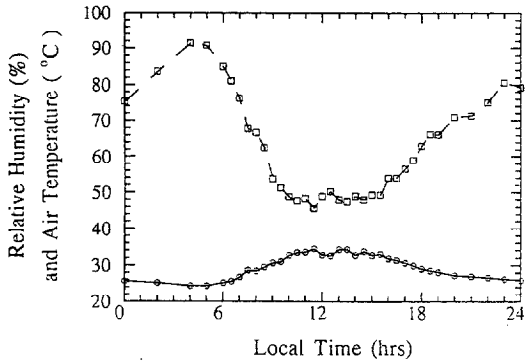

Fig. 7. Air temperature and relative humidity at 1.2 m above surface at the parking lot in the commercial area, – ∘ – air temperature, – □ – relative humidity.

ity at the parking lot in Fig. 7 with that at the grass field in the park in Fig. 3, it is evident that air temperature at the parking lot reached the highest value of 34.5°C at 2 p.m., about 2°C higher than that above the grass surface inside the park at the same time. The relative humidity here reached a maximum of 90% at 5 a.m. and a minimum of 48% at noon, compared with that of 100% and 61%, respectively at the grass field in the park.

In the afternoon, the temperature of the grass surface decreased very quickly and became the same as the air temperature at about 6 p.m.; from 7 p.m. onwards, it was lower than that of the air. Thus at night, the grass surface cooled the atmosphere. On the other hand, throughout the day, the temperature of the asphalt surface was always higher than that of the air, even at night and in the early morning and this surface always heated the atmosphere.

There are various reasons for the higher air temperature in the parking lot compared with that in the grass field inside the park. One of the reasons could be the fact that the place is located inside the commercial area and large values of anthropogenic heat, released due to air conditioning, traffic and other human activities, which might heat the air. However, evaluated values of released anthropogenic heat in the area based on land use and traffic data obtained from the Tama City Government Office indicate that the daily average of anthropogenic heat for this site did not exceed 60 W/m^2. On the other hand, the sensible heat released from the asphalt paved surface (later in Fig. 8(a)) was evaluated at more than 360 W/m^2 at noon, which was about 200 W/m^2 higher than that released from the bare soil surface (Fig. 8(b)). Comparing this value to the 60 W/m^2 of anthropogenic heat (or the values of 245–265 W/m^2 in Section 4.2), it is reasonable to remark that the contribution of the heat released from the pavement surface is larger than that of the anthropogenic heat.

The lower relative humidity in this location is due to the high air temperature and decreased evaporation at the ground surface because of the pavement.

The heated ground surface heats the atmosphere not only by sensible heat exchange, but also by the absorption of longwave radiation emitted from the surface by the atmosphere. The upward longwave radiation emitted by the asphalt pavement surface is 130 W/m^2, higher than that by the bare soil surface as depicted later on in Fig. 8(a,b), and is absorbed within 100 m of the lower atmosphere (Asaeda et al. [2]), increasing air temperature near the ground.

The high air temperature over the asphalt surface in the parking lot, compared with that over the grass surface inside the park, is due to sensible heat exchange with the paved surface, the absorption of longwave radiation emitted from the surface, and anthropogenic heat.

To make a quantitative evaluation of the contribution of the pavement in the commercial and parking area on the heating of the near surface air, and to study in detail the heat balance at each surface, a numerical model developed by Asaeda and Vu [1] has been employed. The heat balance equation at the surface is

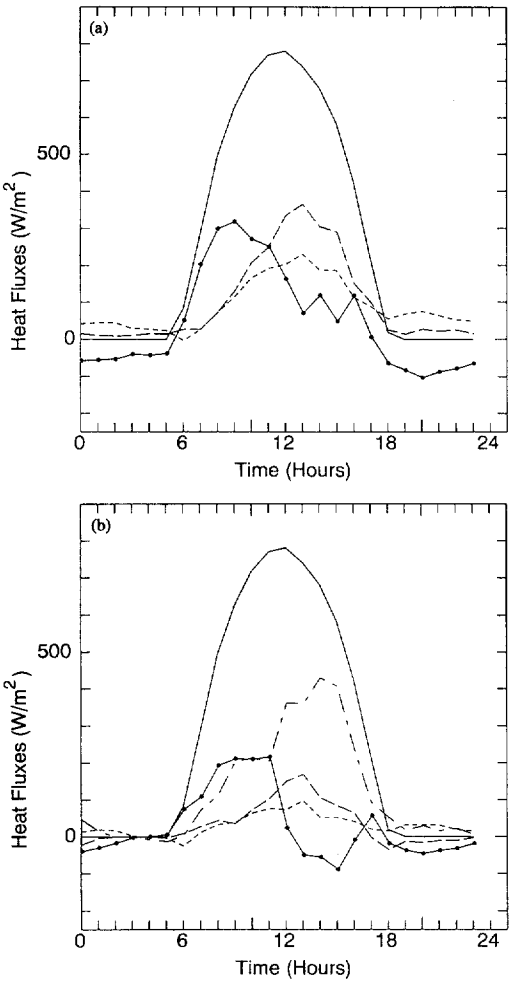

Fig. 8. Components of heat fluxes at the surface of (a) asphalt pavement; (b) the grass field in the park, ——— total downward solar radiation, - - - net upward longwave radiation, – – – sensible heat flux, — — — latent heat flux, – · – downward ground heat flux.

$$-K\frac{\partial T}{\partial z}=S(1-\alpha)+R_{Ln}+H\text{-}L_e \quad (1)$$

where K is the thermal conductivity of the ground surface; T is the temperature of the ground surface; S and R_{Ln} are the solar and net longwave radiation to the surface, respectively; H is the sensible heat flux; L_e is the latent heat flux; and z is the vertical coordinate. The left hand side of Eq. (1) represents the heat flux to the ground at the ground surface.

The solar radiation in Eq. (1) is evaluated based on the measured solar radiation at the grass field and the partitioning of this radiation into direct and diffuse components is estimated following Davies and Hay [4]. The direct solar radiation to the surface under consideration is then estimated based on the solar zenith angle and the height of the obstructing building. The incoming diffuse solar radiation from the sky to the surface is evaluated as the product of total diffuse solar radiation and the sky view factor from the point. Similarly, the incoming longwave radiation to the ground surface is evaluated as the sum of total downward longwave radiation from the sky, multiplied by the sky view factor, and the

longwave radiation emitted by the surrounding walls. The contribution of longwave radiation emitted by the surrounding walls to the net longwave radiation is estimated based on the measured wall surface temperature and the view factor from the surface for the wall. The view factors from the horizontal surface for the sky and walls are determined following Johnson and Watson [10].

It is extremely difficult to determine the sensible and latent heat exchange between the ground surface and the air because of the complexity of the surface conditions at the observational site. However, as the wind velocity, air temperature and relative humidity were measured at many locations, it was attempted to use the values measured at each place to evaluate the heat and moisture exchange between the ground surface and the air at the place. This can minimize possible errors due to the following assumption of local similarity law for the vertical distribution of potential temperature and wind velocity near the ground surface. With this assumption, the sensible heat exchange between the surface and the atmosphere can be evaluated using the following formula (Louis [11]).

$$H=u^*T_p^*=\frac{a^2}{n}U_a(T_p-T_{ps})F_h\left(\frac{z}{z_o},\mathrm{Ri_B}\right) \tag{2}$$

where u_* and T_{p^*} are the scaling velocity and virtual potential temperature, respectively; a^2 is the drag coefficient in neutral conditions; n is a constant equal to 0.74; U_a is the wind velocity at height z; T_p is the virtual potential temperature at height z; T_{ps} is the virtual potential temperature at the surface roughness height z_o; F_h is a function, accounting for atmospheric stability conditions near the ground surface; and $\mathrm{Ri_B}$ is the bulk Richardson number of the layer defined as

$$\mathrm{Ri_B}=\frac{gz\Delta T_p}{\overline{T_p}U_a^2} \tag{3}$$

where $\Delta T_p=T_p-T_{ps}$. The drag coefficient a^2 is defined as

$$a^2=k^2\Big/\left(\ln\frac{z}{z_o}\right)^2 \tag{4}$$

where k is the Von Karman constant.

The atmospheric transport mechanism of water vapor is quite similar to that of the sensible heat (Louis [11], Brutsaert [3]). Thus, it is assumed that the evaporation rate can be described by the same form as Eqs. (2) and (3)

$$e=\rho_a\frac{a^2}{N}U_a(\rho_{vs}-\rho_{va})F_v\left(\frac{z}{z_o},\mathrm{Ri_B}\right) \tag{5}$$

where ρ_a is the air density; ρ_{vs} and ρ_{va} are the specific humidity of air at the surface roughness height z_o and at the screen height, respectively; and F_v is also a function, accounting for atmospheric stability conditions near the ground surface.

The function F_h is supposed to have the form (Louis [11])

$$F_h=\begin{cases}1-\dfrac{b\mathrm{Ri_B}}{1+c|\mathrm{Ri_B}|^{1/2}} & \text{for unstable case}\\[2ex] \dfrac{1}{(1+b'\mathrm{Ri_B})^2} & \text{for stable case}\end{cases} \tag{6}$$

The functions F_h and F_v are assumed to have the same form. Thus,

$$F_v=C_1^*F_h \tag{7}$$

where the coefficient C_1^* is assumed constant and can be determined from the calibration of the model by comparing the computed and measured temperatures of the soil surface until a best fit between them. C_1^* was determined by Asaeda and Vu [1] as 0.68.

In Eq. (6), $b=2b'=9.4$, and c is defined as

$$c=C^*a^2b\left(\frac{z}{z_o}\right)^{1/2} \tag{8}$$

where C^* is a constant equal to 5.3 for both vapor and heat fluxes (Louis, 1979). Once F_t is determined, the turbulent sensible heat flux can be determined as

$$H=\rho_aC_pF_t=\rho_aC_p\frac{a^2}{N}U_a(T_p-T_{ps})F_h\left(\frac{z}{z_o},\mathrm{Ri_B}\right) \tag{9}$$

and the latent heat as

$$\begin{aligned}L_e &=L\rho_a\frac{a^2}{N}U_a(\rho_{vs}-\rho_{va})F_v\left(\frac{z}{z_o},\mathrm{Ri_B}\right)\\ &=L\rho_a\frac{a^2}{N}U_a(\rho_{vs}-\rho_{va})C_1^*F_h\left(\frac{z}{z_o},\mathrm{Ri_B}\right)\end{aligned} \tag{10}$$

Fig. 8(a–b) depict components of heat fluxes at the asphalt pavement surface and the surface of the grass field inside the park, respectively. As seen in Fig. 8(a), for the asphalt pavement, the ground heat flux peaks at 9:00 a.m. with a value of about 320 W/m^2 and remains positive until 5:00 p.m. This large ground heat flux is released in the early evening to the atmosphere in the form of sensible heat and upward longwave radiation. The upward transfer of sensible heat and net upward longwave radiation peak at 1:00 p.m. with values of 370 W/m^2 and 230 W/m^2, respectively. The sensible heat directly heats the air while the upward longwave radiation is absorbed within a thin air layer near the ground surface (Asaeda et al. [2]), affecting the near surface air temperature. Since the asphalt surface is always hotter than the overlying air throughout the day and night, the surface always heats the air even late a night, contributing to the formation of the so called 'nocturnal urban heat island'.

Fig. 8(b) shows that for the grass surface, the largest portion of net radiation to the surface is converted to latent heat. The latent heat increases with time from the morning, and at 12:00 a.m. its value is greater than 360 W/m^2. At this time, with the net solar radiation of 610 W/m^2 reaching the surface, only 150 W/m^2 is converted to sensible heat and 75 W/m^2 is converted to net upward longwave radiation. The ground heat flux at this time is only 25 W/m^2. At 1:00 p.m., the latent

heat is 360 W/m^2 while the sensible heat and net upward longwave radiation are 170 W/m^2 and 100 W/m^2, respectively. Thus the cooling of the grass surface is mainly due to latent heat and the direct heating of the air by sensible heat, while the net upward longwave radiation is rather small. The latent heat peaks at 2:00 p.m. at a value of 420 W/m^2. From 5:00 p.m. onwards, the temperature of the grass surface becomes lower than that of the air, and the surface begins to cool the air due to downward transfer of sensible heat. The ground heat flux peaks at 11:00 a.m. with a value of 215 W/m^2, becoming negative at 1:00 p.m. when cooling of the soil surface begins.

Fig. 9(a) depicts contour lines of the air temperature constructed from measured data at 1.2 m above surface for all observational points at 00:00 a.m. The contour lines are drawn by interpolating air temperature recorded at each observational point. From Fig. 9(a), even at this time, the air temperature difference between the coolest and hottest places amounted to 1.5°C. The highest air temperature at the Tama Central Station and a road in a housing area in the South-East of the park was 25.7°C. The reason for high air temperatures here is the heat released from paved surfaces and anthropogenic heat released mainly due to air conditioning. The lowest air temperature inside the park was 24.2°C. At this time, there is no predominant wind and the cooling effects by the park extends almost equally in all directions. From the figure, one can see that the influence area extends only about 100 m from the park.

Fig. 9(b) depicts contour lines of air temperature at 9:00 a.m. As in the figure, the air temperature at the hottest place over a parking lot in the commercial area to the North of the park had reached 30.5°C, 2.5°C higher than that at the coolest place in the park. Since there was no obstruction to the solar radiation receipt of the parking lot, the surface temperature of the asphalt pavement had reached more than 40°C; and the most likely candidate which contributes to the high air temperature in this place is the sensible heat released from the pavement surface. However, since this place is located in the commercial area, anthropogenic heat released by air conditioning, traffic and other commercial activities can contribute significantly to the heating of air here. The air temperature measured in Partenol street, which is also located in the center of the commercial area is not much higher even with the expected high anthropogenic heat flux. One reason for this is in the morning, the street is in the shade due to high rise buildings located on both sides of this wide street. This phenomenon has been investigated by Vu et al. [18], Swaid and Hoffman [17], Sharlin and Hoffman [16]. The other reason for the cool air in the Patenol street is because of the influence of the park. At this time, there was a moderate South-East wind and as in the Fig. 9(b), and a cool area in the North-West of the park was due to this wind. The cooling effect of the park extended about 700 m beyond the park boundary.

At 12 a.m., the pattern of temperature distribution in the city is rather complicated, as shown in Fig. 9(c). The hottest place is now at the northern entrance of the park with air temperature reaching 33.7°C. This open space is located overhead a heavy traffic street and is surrounded by offices and commercial buildings. The continuous heating of the pavement surface by solar radiation and the release of anthropogenic heat contributes to the high air temperature here.

A cool spot is observed at the Tama Central Park where air temperature reached 31.5°C. The park was exposed to solar radiation throughout the morning, but evaporation from the grass surface and trees and the shading effects of trees caused low ground surface temperature, and consequently low air temperature. The air temperature difference between the park and the hottest area in the town is 2.2°C. Like that in Fig. 9(b), there was a cool area just in the North-West of the hot area in the northern entrance of the park. At this time, the South-East wind became very strong, and it can be observed that due to this wind, the influence area of the park can extend to a distance of about 1 km in the North-West direction, from the park until the Tama Central Station.

Other hot areas at this time are located in the North-East and the South of the park where the air temperature reached more than 33.5°C. A steep horizontal air temperature gradient is observed in the South-East, East and North of the park.

The cooling effect of the park is clearly observed in the early afternoon as shown in Fig. 9(d), which depicts the contour lines of air temperature at 2:00 p.m. The park now becomes a cool island surrounded by hot areas. The difference in air temperature between the park and the hottest place at the Tama Central Station is more than 2°C. As the wind direction has changed to that from the South, the influence of the park in the North-West direction was diminished. The cool area at this place now became a hot area. This is because the heating from the surface of the parking lot and artificial heat released due to traffic and extensive air conditioning at this time prevailed over the cooling effect. However, the influence area of the park now shifted to the Partenol street. As stated before, this is a busy commercial street with a wide paved road, which is fully exposed to solar radiation from 12:00 a.m. At this time, there is also an extensive heating due to air conditioning and the hot ground surface. However, even with this heating, air temperature in the street reached only 32°C, well below that in the surrounding areas. The hot area at the northern entrance of the park is also much weaker than it was at 12:00 a.m.

4. Effect of the park on thermal environment and energy use

4.1. Effect of the park on the thermal comfort

The effects of vegetation on the thermal environment in the urban area can be evaluated based on thermal comfort analysis. In this study, this is done by employing a two-nodes model for the human physiological regulatory response, proposed by Gagge et al. [25,26]. The model will be briefly described here.

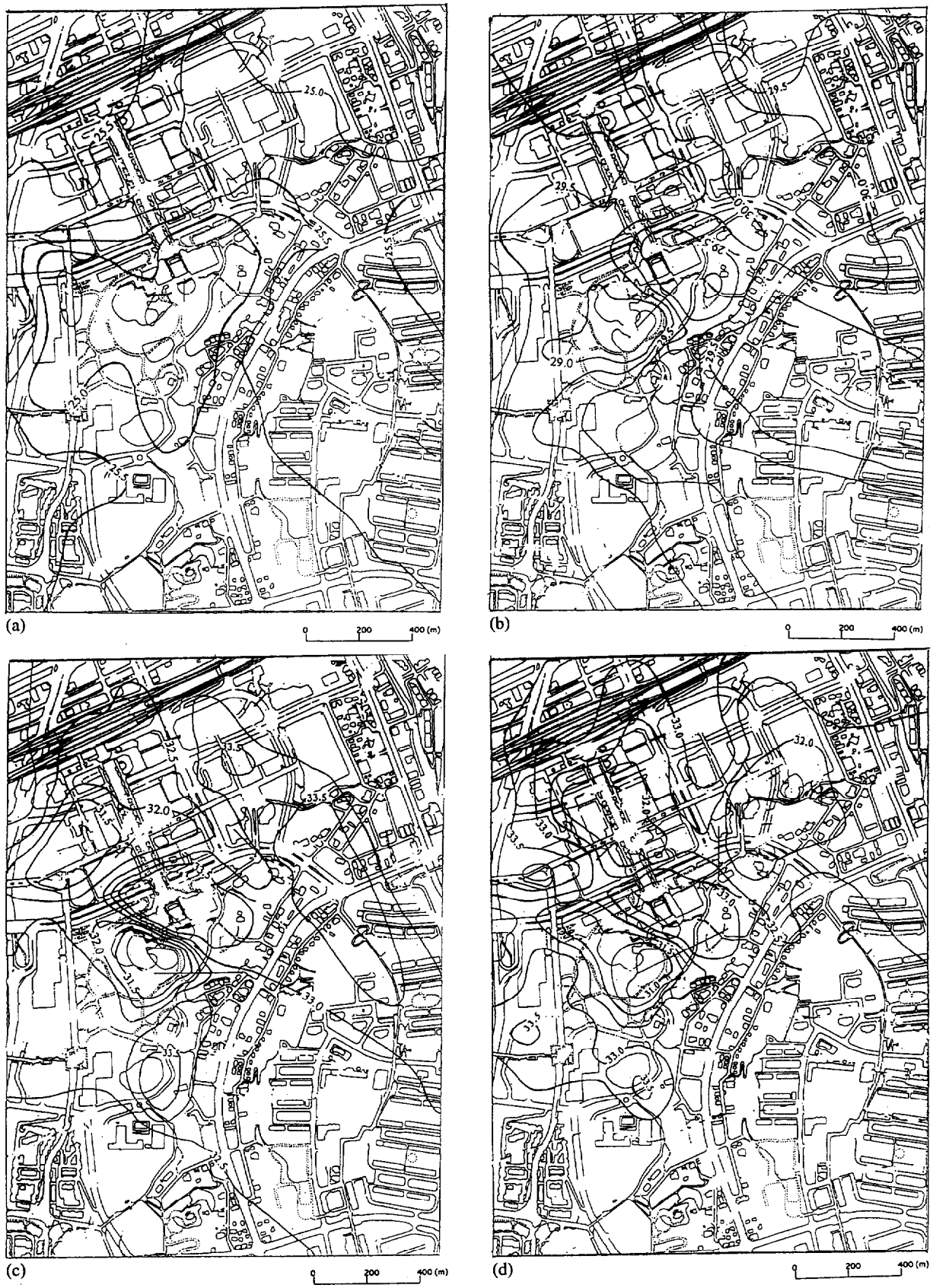

Fig. 9. Contour lines of air temperature at 1.2 m above surfaces at (a) 00:00 a.m., (b) 9:00 a.m., (c) 12:00 a.m., (d) 2:00 p.m.

The heat exchange between the skin and the environment at the skin surface H_{sk} is described by the heat balance equation as

$$H_{sk}=h'(T_{sk}-T_o)+wh_e'(P_{ssk}-P_{sdp}) \quad (11)$$

where h' is the combined heat transfer coefficient over the temperature gradient; T_{sk} is the skin temperature; T_o is the operative temperature, defined as the average of ambient air temperature and the mean radiant temperature (MRT), weighted by their respective linear heat transfer coefficient h_c and h_r; w is the skin wetness; h_e' is the latent heat transfer coefficient; P_{ssk} is the saturated vapor pressure at skin; and P_{sdp} is the ambient vapor pressure.

The heat flow to the skin surface from the body core is expressed as

$$H_{sk}=M-W-(E_{res}+C_{res})-(S) \quad (12)$$

where M is the metabolic heat; W is the accomplished work; E_{res} and C_{res} are latent and sensible heat exchange by respiration, respectively; and S is the body heat storage.

The thermal comfort is evaluated by the Predicted Mean Vote (PMV), proposed by Fanger [27] as

$$PMV=\alpha[H_{sk}-h'(T_{sk}-T_o)-E_{diff}-E_{comf}] \quad (13)$$

where E_{diff} is the evaporative heat loss caused by diffusion of moisture through the skin and approximately 6% of the maximum possible evaporative cooling E_{max} from the skin surface when the skin wetness $w=1$; and E_{comf} is the evaporative loss by sweating that occurs during the state of comfort and is evaluated by Fanger [27] as:

$$E_{comf}=0.42(M-W-58.2) \quad (14)$$

The maximum evaporative heat loss E_{max} from the body surface can be evaluated as (Gagge et al. [25])

$$E_{max}=\kappa h_c[P_{sk}-P_{dew}] \quad (15)$$

where κ is the Lewis relation and h_c is the convective heat transfer.

Values of the coefficients in the model are selected according to Kanda and Tsuchiya [19], [20], Gagge et al. [25,26] and Fanger [27].

The model has been employed for the analysis of thermal comfort in the area. It found that at 12 a.m., inside the park, the PMV for a walking person is 2.6. The PMV for the same person in the upwind direction of the park is 3.2 and the corresponding value of PMV in the downwind direction of the park is 2.8.

Thus, with the presence of the park, a significant decrease in the predicted mean vote is achieved, and the thermal environment in the area is improved.

4.2. Impacts of the park on energy use

Konopacki et al. [22], Meier and Taha [21] showed that the for cities in the United States, a 1–2°C reduction in space-averaged air temperature (at around 2 p.m. local time) leads to a decrease of up to 10% in peak energy demand. In terms of annual costs of energy use, results of computations by the authors suggested net savings in the order of US$10–35 per 100 m^2 of roof area depending on building type and region.

In this study, a model proposed by Vu et al. [24] was employed for the evaluation of the reduction in air conditioning energy caused by the park. The model is a coupling of a meso-scale model for the urban climate which allows a computation of the heat exchange between buildings and the air in the urban canopy layer and a model for the evaluation of building air conditioning energy. In the model, the conduction heat flux to rooms of a building through walls and roof is evaluated by solving the heat conduction equation for the walls, roof with an assumed constant room air temperature; and the air conditioning energy is evaluated based on the heat exchange between walls, roof with room air, other heat loads in the room due to machines, lights and human body, and the cooler's coefficient of performance (denoted as COP, a ratio of pumped heat to utilized electricity).

Vu et al. [24] and Tanaka et al. [23] found that for air-cooling type heat pumps or building multi-purpose type heat pumps, COP decreases with increasing ambient air temperature, and is a function of partial load of the heat pump (defined as the ratio of needed electricity and the capacity of the heat pump). Multi-purpose type heat pumps are commonly used for room cooling in commercial and office areas. Since the area under the influence of the park in this study is a commercial and office area, this type of heat pump with the capacity of 13 HP is used for the analysis.

Buildings used for the analysis are assumed as modern four-storey ones with a fixed room temperature of 26°C. This room temperature is typical for commercial and office rooms in Japan during summer (Vu et al. [24]). The building ratio (ratio of the ground surface covered by buildings to the total land surface) is assumed as 0.5 and the average width of each building in a mesh is 20 m. Results of computations shows that at noon with an outside air temperature of 33.5°C and roof level wind velocity of 3 m/s, the total conduction heat to the room through walls and roof is 52 W/(m^2 ground surface). This is about a half of other heat loads in the room due to machines, lights and human body for this type of building, which is approximately equal to 125 W/(m^2 ground surface). Thus, the total heat to be pumped out of the building amounted to 177 W/(m^2 ground surface).

The COP, computed from outside air temperature and the heat pump partial load for this case is 3.3. Thus, the electricity needed for the heat pump is 54 W/(m^2 ground surface) and the total anthropogenic heat released to the air is 224 W/(m^2 ground surface).

With the outside air temperature of 31.5°C, the computed conduction heat flux to the room is 42 W/(m^2 ground surface). With a COP of 3.6, the evaluated electricity needed for the heat pump becomes 46 W/(m^2 ground surface) and the total anthropogenic heat released to the air becomes 223 W/(m^2 ground surface). Therefore, 8 W/(m^2 ground surface), or 16 W/(m^2 build up area) of electricity for air cooling can be saved, and the reduction of anthropogenic heat

release can improve air quality in the area. Thus, it can be found that a saving of almost 15% in air cooling electricity at noon is saved. This is a little large than that evaluated by Konopacki et al. [22], and Meier and Taha [21]. It must be emphasized that the buildings used for this study are official buildings, and the conduction heat to the room is larger for residential buildings.

From observational results, it is found that the area of influence of the park is almost 0.5 km^2. Thus, within 1 h, from 1 to 2 p.m., with the presence of the park, 4000 kW h of electricity can be saved, and air quality in the area can be improved.

The price for electricity in Japan is approximately ¥22 per kilowatt hour for summer. With 4000 kW h of saved electricity, ¥88 000, or roughly, US$650 can be saved within 1 h.

5. Conclusion

From observational results, it is found that even though small, the Tama Central Park is significantly cooler than the surrounding area during the day and at night. With strong local southern winds during the day, it is expected that the cool air from the park, being brought to the town, can significantly contribute to the reduction of the heat intensity in the town.

The presence of the park can significantly improve the thermal environment in the town. It is estimated that 4000 kW h of electricity for cooling, or US$650 can be saved within 1 h from 1 to 2 p.m. of a hot summer day. Also, the anthropogenic heat released to the air can be reduced.

Acknowledgements

The authors are grateful to Professor Milo Hoffman of National Building Research Institute, Technion Institute of Technology, Israel, and two referees for their careful reading of the first draft of this paper and provided many useful suggestions, even English correction. Many thanks are given to Dr. Tuan Pham of the University of New South Wales, Australia for English checking of the draft and many useful suggestions. The contribution of Dr. Murakami of Nihon Koei, Dr. Fujino of Saitama University, many people from Nihon Koei and graduate and undergraduate students of Saitama University in the observation and data processing are greatly appreciated.

References

[1] T. Asaeda, T.C. Vu, The subsurface transport of heat and moisture and its effects on the environment: a numerical model, Boundary-Layer Meteorol. 65 (1993) 159–179.

[2] T. Asaeda, T.C. Vu, A. Wake, Heat storage of pavement and the effects on the near surface atmosphere, Atmospheric Environment, Part B, Urban Environment 30 (1996) 413–427.

[3] W. Brutsaert, Evaporation into the Atmosphere, Theory, History and Applications, D. Reidel Publ., 1984, 299 pp.

[4] J.A. Davies, J.E. Hay, Calculation of the solar radiation incident on a horizontal surface, in: J.E. Hay, T.K. Won (Eds.), Proceedings of the First Canadian Solar Radiation Data Workshop, 1978, 32–58.

[5] D. Doll, J.K.S. Ching, J. Kaneshiro, Parameterization of subsurface heating for soil and concrete using net radiation data, Boundary-Layer Meteorol. 32 (1985) 351–372.

[6] B. Givoni, Impact of planted areas on urban environmental quality: a review, Atmospheric Environment 25B (1991) 289–299.

[7] Y. Harazono, S. Teraoka, I. Nakase, H. Ikeda, Effects of rooftop vegetation using artificial substrates on the urban climate and the thermal load of buildings, Energy and Buildings 15–16 (1991) 435–442.

[8] T. Honjo, T. Takakura, Simulation of thermal effects of urban green area on their surrounding areas, Energy and Buildings 15–16 (1991) 443–446.

[9] A. Hoyano, Climatological uses of plants for solar control and the effects on the thermal environment of a building, Energy and Building 11 (1988) 181–199.

[10] G.T. Johnson, I.D. Watson, The determination of view-factors in urban canyons, J. Clim. Appl. Meteorol. 23 (1984) 329–335.

[11] J.-F. Louis, A parametric model of vertical eddy fluxes in the atmosphere, Boundary-Layer Meteorol. 17 (1979) 182–202.

[12] T.R. Oke, The energetic basis of urban heat island, Quart. J. R. Met. Soc. 108 (1982) 1–24.

[13] J.H. Parker, The effectiveness of vegetation on residential cooling, Passive Solar J. 2 (1983) 123–132.

[14] J.H. Parker, The use of shrubs in energy conservation planting, Landscape J. 6 (1987) 132–139.

[15] J.H. Parker, The impact of vegetation on air conditioning consumption, Proc. Conf. on Controlling the Summer Heat Island, LBL-27872 (1989) 46–52.

[16] N. Sharlin, M.E. Hoffman, The urban complex as a factor in the air temperature pattern in a mediterranean coastal region, Energy and Buildings 7 (1984) 149–158.

[17] H. Swaid, M.E. Hoffman, Prediction of urban air temperature variations using the analytical CTTC model, Energy and Buildings 14 (1990) 313–324.

[18] T.C. Vu, T. Asaeda, M. Ito, S. Armfield, Characteristics of wind field in a street canyon, J. Wind Eng. Aero-dynamics 57 (1995) 63–80.

[19] Chronological Table of Science (in Japanese), p. 266 (in Japanese).

[20] M. Kanda, N. Tsuchiya, Field observation and analysis for estimating thermal load on a human body, Annual J. of Hydraulic Engr., JSCE 38 (1994) 419–424.

[21] A. Meier, H. Taha, Mitigation of urban heat islands: meteorology, energy, and air quality impact, Proc., Int. Symp. on Mornitoring and Management of Urban Heat Island, Japan, 1997, 124–163.

[22] S. Konopacki, H. Akbari, S. Gabersek, L. Gartland, M. Moezzi, M. Pomerantz, Energy and cost benifits from light-colored roofs in 11 U.S. cities, Lawrence Berkeley National Laboratory Report LBL-39433, Berkeley, CA, 1996.

[23] M. Tanaka, M. Ozawa, Y. Ashie, A practical use of vaporization heat of building materials for the improvement of urban climate, Part 4: Thermal environmental load around buildings from air conditioners, Japanese Conference on Remote Sensing, in Japanese, 1997, 1249–1252.

[24] T.C. Vu, Y. Ashie, T. Asaeda, Analysis of building air conditioning energy during summer season, in preparation for submission to Energy and Building.

[25] A.P. Gagge, J.A.J. Stolwijk, Y. Nishi, An effective temperature scale based on a simple model of human physiological regulatory response, ASHRAE Semiannual Meeting in Philadelphia, PA, 1970, 247–262.

[26] A.P. Gagge, A.P. Fobelets, L.G. Berglund, A standard predictive index of human response to the thermal environment, ASHRAE Transactions, Part 2B 90 (1986) 709–731.

[27] P.O. Fanger, Thermal Comfort Analysis and Applications in Environment Engineering, Danish Technical Press, 1970.